

Flight Stability of Droplets in an Electrostatic Ink-Jet Printer

*Shogo Matsumoto, Tomohiro Inoue and Junichi Matsuno
Mechanical Engineering Research Laboratory, Hitachi Ltd., Ibaraki, Japan
Nobuhiro Harada and Kiyosi Sano
Home Appliances Division, Hitachi Ltd., Ibaraki, Japan*

Abstract

We describe the flight stability of droplets in an electrostatic ink-jet printer. The droplets are charged and fly near to other particles, and they therefore interact with the other particles and deviate from their expected trajectories. These interactions are a major cause of droplet-placement errors in high-speed printing. To understand the cause of such errors, we observed flying droplets, measured the charges in each droplet, and modeled the flight dynamics in a simple system. We discuss the causes of placement errors based on observations, measurements, and numerical analysis, including an analysis of the effects of electrostatic repulsion and the interactions resulting from aerodynamic forces. A method of reducing droplet-placement error is also discussed, and its effectiveness is confirmed.

Introduction

Electrostatic ink-jet printers (IJP) can print on many kinds of media from a long distance (working distance). Because of this feature, they are used in industrial marking equipment such as that used to print the production date on cans of soft drinks, and so on. In recent years, there has been a demand for higher printing speed and better print quality to reduce manufacturing costs.

Electrostatic IJPs generate droplets by vibrating an ink stream that is shot continuously from a nozzle, as shown in Figure 1. Voltage is applied via a charge electrode, and individual droplets are charged depending on the data being printed. The charged droplets are subjected to a deflection force, applied by causing them to fly between two deflection electrodes on the way to the target. On the other hand, non-printing droplets are not deflected; they fly straight, and are caught by a gutter and reused.

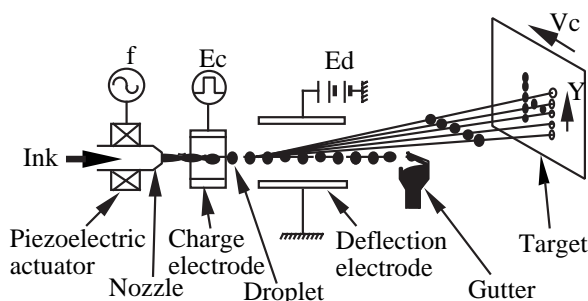


Figure 1. Schematic view of IJP

Because the droplets are charged, they are subject to several forces during flight, as shown in Figure 2. At the moment of charging, charge errors occur and the charge of a droplet becomes smaller than the expected value due to the influence of the preceding droplet. Furthermore, during flight, droplets are affected by various aerodynamic forces (which depend on the interactions between droplets), and by electrostatic forces due to the other droplets. These forces are complexly mixed and combine to cause droplet-placement errors. Countermeasures against droplet-placement errors are difficult because there are a variety of interactions that change according to the arrangement of droplets. Formerly, we reduced droplet-placement errors by interspersing them with dummy droplets to reduce their interactions.¹ However, in high-speed printing, we can not afford to produce such dummy droplets, because we need to use every droplet. Droplet-placement errors occur as shown in Figure 3 when dummy droplets aren't used.

It is extremely effective to consider the relationship between the arrangement of the flying droplets and print quality in an integrated model. However, most previous investigations focused mainly on localized phenomena such as the mechanism of droplet formation.²⁻⁵ This being the case, countermeasures against droplet-placement error depended on coefficients of compensation that were obtained experimentally,¹ so such countermeasures never became common for use in high speed bar-code printing and with new characters and patterns.

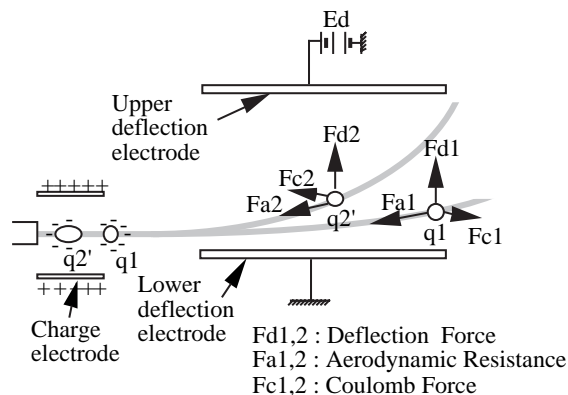


Figure 2. Effects of interaction of electrostatic repulsion and aerodynamic forces

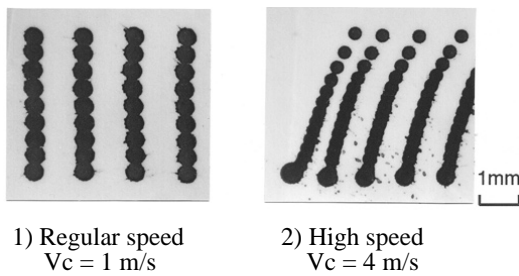


Figure 3. Drop placement error

In this study, to solve these problems, we observed flying droplets, measured the charge in each, and modeled the flight dynamics in a simple simulation system. By carrying out experiments and analysis in support each other, we will elucidate the cause of droplet-placement errors.

Observation of Flying Droplets

Observation Apparatus

To understand the cause of droplet-placement errors, we constructed an ink-jet observation apparatus (Figure 4) and observed the arrangement of flying droplets. In this apparatus, a stroboscope is flashed at the time voltage is applied to the charge electrode, in order to observe droplet placement during each line of printing. We can obtain several pieces of information (such as the velocity of the droplets) by computation from the data obtained in these observations.

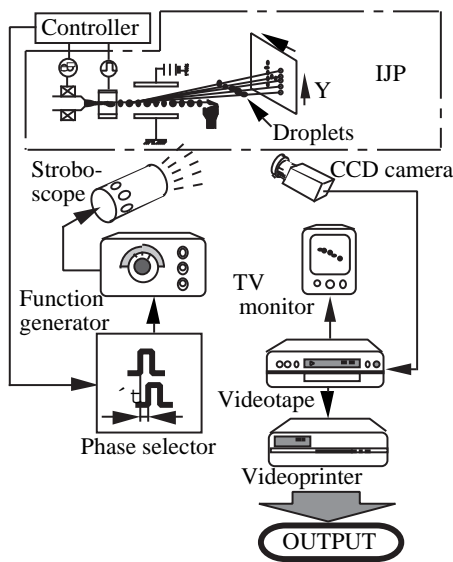


Figure 4. Schematic view of ink-jet observation apparatus

Relationship Between Flight Formations and Droplet-Placement Errors

Droplet placement during vertical-line printing is shown in Figure 5, as observed using the observation apparatus. In this picture, the deflection electrodes are horizontal and parallel and the droplets are flying toward the right. The first droplet catches up with the second droplet and

they merge. The last droplet flies slower than any other droplets. Also observed was the curved (non-linear) droplet-flight formation.

The reason for the curved printed lines (Figure 3) is thought to be the velocity differences between droplets in the same line.

We calculated the distribution of velocities from the stroboscopic observation, and prediction the printed-line shape using this distribution. We then confirmed that this shape was the same as that produced by the actual droplet-placement errors, as shown in Figure 3. We will now discuss the reasons for this distribution of velocities, focusing on the case shown in Figure 5. (The IJP specifications are shown in Table 1.)

Table 1. IJP specifications

Diameter of nozzle d_j	65 μm
Frequency f	68 kHz
Initial velocity of droplet v_0	20.2 m/s
Deflecting electric field E	0.9 kV/mm

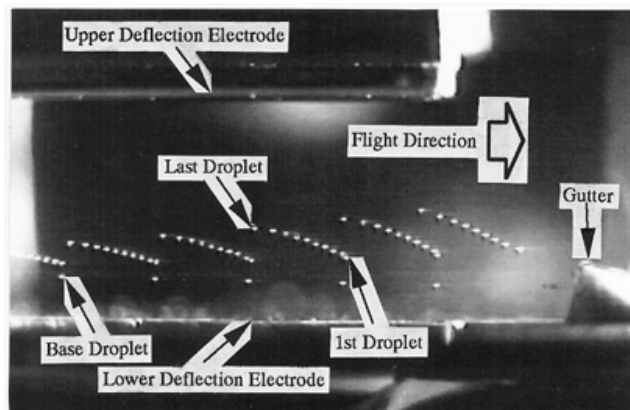


Figure 5. Drop placement during printing of vertical lines (video observation)

Measurement of Charges

Charge-Measuring Apparatus

It is important to recognize the influence of charge error, which results from interactions with the previous droplet during the charging period, because it directly influences printing quality. To study the droplet-placement error which depends on charge error, we built a small charge-measuring apparatus and measured the charge in each droplet. In this device, each charged droplet is caught on an earthed catch plate, and then the current is measured and the charge calculated. This equipment is capable of measuring the charge in each droplet due to the use of an operational amplifier with high impedance and low input-bias to amplify the current. Calibration of output voltage with input current is carried out by connecting the droplet catch-plate with capacitor with a known capacitance.

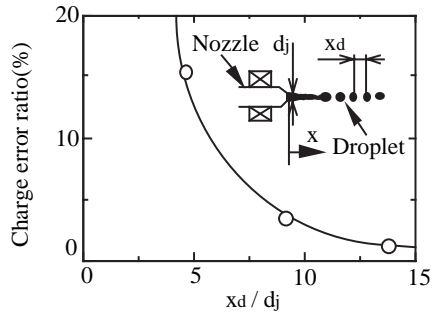


Figure 6. Relationship between charge-error ratio and drop placement

Measurement of Charge Error

To estimate the charge error, charge in droplet is measured in the case of a 2-drop fly. In this experiment, the inter-droplet distance dx is varied. Measured data are shown in Figure 6. In this figure, droplet distance xd is expressed as a multiple of nozzle diameter d_j , and the charge-error ratio is defined as ratio of charge of first droplet to the difference of the charge of the second droplet from its expected value. The graph shows that charge error gets worse with reduced droplet spacing, which makes it easy to understand why droplet-placement error becomes worse in high-speed printing in which we can not use any dummy droplets. Charge error can be controlled by applying modified voltages to the charge electrode. The appropriate modified voltages can be obtained based on the voltage applied to the preceding droplet.

Numerical Analysis of Flight Dynamics of Droplets

Analysis

We will now discuss a numerical analysis of droplet flight dynamics to give insight into the mechanism of droplet-placement error and to study effective methods of reducing it. The flow of our analysis is shown in Figure 7. First, the charge on each droplet is calculated in consideration of the ink spray velocity, the diameter of the droplets, and charge errors due to printing conditions. Next, the acceleration affecting the droplet at each instant of time is calculated, and integrated over all the flight paths to obtain the instantaneous flight trajectory. The method of estimation used for each item will be discussed next.

1. Droplet Diameter

We can obtain the relationship between the diameter d_j of the nozzle and the diameter d of the droplets as follows,⁶ since the mass of the ink is conserved:

$$d = A_1 d_j ((3/2)(\lambda / d_j))^{1/3} \tag{1}$$

Here, λ is the distance between droplets, A_1 is a correction coefficient. From the observation of flying droplets under the conditions shown in Table 1, we obtained $A_1 = 0.931$.

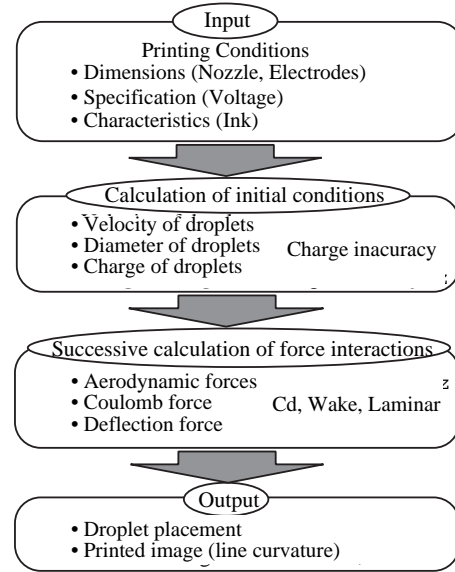


Figure 7. Flow of analysis

2. Droplet Charge

The charge q in a droplet at the charge electrodes is given by equation (2) by approximating the 2 panels of charge electrodes with infinite planes and the droplets with a solid system.⁶

$$q = 2\pi A_2 \epsilon_0 \lambda V_s / \ln(4d_s / \pi d) \tag{2}$$

Here, ϵ_0 is the permittivity of a vacuum, V_s is the charging voltage, d_s is the distance between the two charge electrodes, and A_2 is a correction coefficient. From the measurement of charge q , we obtained $A_2 = 1.054$.

3. Deflection Force

Droplets are charged at the charge electrodes and undergo deflection force F_1 during their flight through the electric field between the deflection electrodes.

$$F_1 = q E \tag{3}$$

Where, E is the strength of the electric field between the deflection electrodes.

4. Coulomb Force

Charged droplets are used for IJP and are subject to Coulomb force F_c due to the preceding and succeeding droplets.

$$F_c = q_1 q_2 / (4 \pi \epsilon_0 r^2) \tag{4}$$

Here, r is the distance between successive droplets.

5. Aerodynamic Forces

Droplets fly through air and are therefore affected by aerodynamic forces. Aerodynamic force F_a can be defined as follows, under the approximation of droplet shape as perfect spheres of diameter d .⁷

$$F_a = Cd (1/2)\rho v^2 \pi / 4 d^2 \tag{5}$$

Where, C_d is the coefficient of drag, and ρ is the density of air. When the Reynolds number of the air is less than 1, the equation of Oseen is applicable, but when the Reynolds number is over 200, as is usually the case in IJP, there is no theoretical relationship between it and C_d . In this study, for simplicity and useful analysis (discussed later), we will neglect higher velocities, and use Oseen's equation:

$$C_d = A_3 ((B_1 / Red + B_2), \tag{6}$$

where, $Red = v d / \nu$ and ν is kinematic viscosity, and B_1 and B_2 depend on Red as follows: when $Red \leq 1$ then $B_1 = 24$, and $B_2 = 4.5$ (equal to Oseen's equation); when $1 < Red \leq 2$ then $B_1 = 27$ and $B_2 = 1.5$; and when $2 < Red \leq 200$ then $B_1 = 60$ and $B_2 = 0.5$.

Next we obtain A_3 from observation of droplets in flight. Given that droplets are affected by both aerodynamic and deflection forces, we can obtain equation (7) from equations (3) through (6).

$$dv / dt = -G (v^2 + 2 Q_1 v + Q_2), \tag{7}$$

where, G , Q_1 , and Q_2 are coefficients that depend on printing conditions, and Q_2 is a function of the vector that represents the flight direction of the droplet. In this study, for simplicity, we will consider Q_2 as a constant, solve the differential equation by separation of variables, and thus determine the relationship between time t and velocity of droplets v using A_3 . We can measure velocity v at time t from our observations, and thus determine that $A_3 = 1.116$.

Treatment of Interactions of Droplet in Aerodynamic Force

When droplets fly continuously in the air, the aerodynamic forces applied to a droplet are influenced by the preceding droplet as mentioned above. In this section, we consider the influence of base droplets (droplets that are not deflected) and preceding droplets on the droplets that follow.

1. Effects of Base Droplets

All droplets in non-printing mode and printing-mode droplets that are not used are not charged, and thus fly straight into the gutter. The air around these "base droplets" has a velocity distribution reflective of its being dragged with these droplets. In this study, we will consider this flow to be stable. Approximating this phenomena as a laminar flow near an infinite plane gives us our velocity distribution.

Laminar flow near the plane if the velocity at infinite distance from the plane is u_∞ , can be represented as follows,⁸

$$u/u_\infty = (1/2)f'(\eta) \tag{8}$$

Where,

$$f'(\eta) = \alpha \eta/1! - \alpha^2 \eta^4/4! + 11 \alpha^3 \eta^7/7! - \dots \tag{9}$$

In this study, we adopt the value $\alpha = 1.32824$ as numerically integrated by Topfer using the Kutta theorem.⁸ By measuring the position at which droplets begin to be influenced by aerodynamic forces, we arrive at $u/u_\infty = 1/2$.

Thus from equation (8), we obtain $f'(\eta)=1$, and get $\eta = 0.77192$ via equation (9). Then,

$$\delta_1 = 2 \eta (\nu x/u_\infty)^{1/2} \\ (\approx) 0.54384(\nu x/u_\infty)^{1/2}.$$

In this study, we consider the velocity of a laminar flow of thickness δ_1 , to be same as the velocity of the base droplets. We will now consider the effects of these base droplets by calculating the aerodynamic forces that affect droplets flying in this layer from the difference between velocities of the droplets and the air flowing in the layer.

2. Effects of Wake

Wakes form behind flying droplets as shown in Figure 8. When we consider a droplet as a sphere, the width b of the wake increase in proportion to $x_w^{1/3}$ increase and the maximum velocity reduction u_{max} decreases in proportion to $x_w^{-2/3}$.⁷ In this study, we set

$$b = d (1 + A_4 x_w)^{1/3}, \text{ and} \tag{11} \\ u_{max} = v (2d/(2d + A_5 x_w))^{2/3},$$

where, A_4 and A_5 are coefficients that we obtained experimentally.

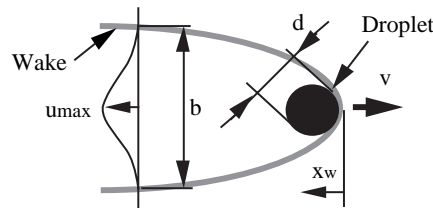


Figure 8. Wake

From observation of two flying droplets following the same path, the drag C_d of the latter droplet is obtained in the same way as in the discussion of aerodynamic forces in section 5. And by considering the value of u_{max} that is caused by the preceding droplet, we can obtain A_5 . Furthermore, we obtain A_4 from observations of whether or not the 2 droplets merge when the charge of following droplet is varied. From the 2-drop fly experiment, we obtained $A_4 = 0.05$ and $A_5 = 1.00$.

In this study, by simplifying to consider the velocity of the flow within the wake of width is b to be equal to u_{max} everywhere, we can consider the effect of the wake to be the same as in the case discussed in the Introduction.

Analysis Conditions

Numerical analyses of the flight dynamics of droplets was carried out according to the method discussed above. In the next section, this analysis is carried out for the conditions shown in Table 1, which correspond to the printing conditions photographed for Figure 5.

Interaction in 2-drop Fly

When droplets fly continuously, a non-linear region will be observed where merge and scatter occur because of interactions between droplets. In this region, the motion of droplets is uncontrollable and improvement of printing quality is difficult. So that reason, recognition of this region is important when designing of a printer. To discern this region, a 2-drop fly print experiment was carried out. In this experiment, the voltage applied to the charge electrode for the first droplet was fixed at 248 V and that applied for the second droplet was varied to observe the effects on the flying droplets. A numerical analysis was also carried out. In this study, we will discuss the interaction between droplets in terms of deflection. The result of the experiment are shown in Figure 9. An approximately linear decrease in the deflection of the second droplet can be seen; this is caused by charge error. There is also a merge area, where the two droplets merge in the region where the charges are approximately the same. This merge area and the scatter area that is formed next to it clearly define the non-linear region. Next, analysis for the case of vertical-line printing is carried out using the same technique.

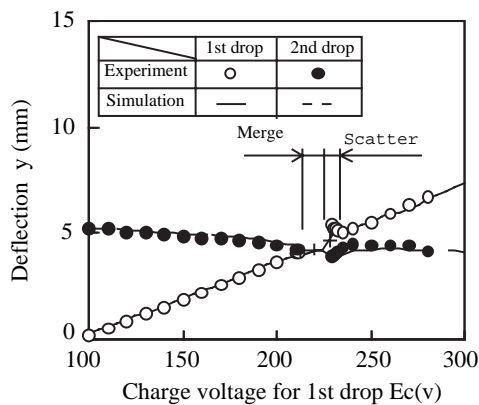


Figure 9. Interaction of flight of two drops

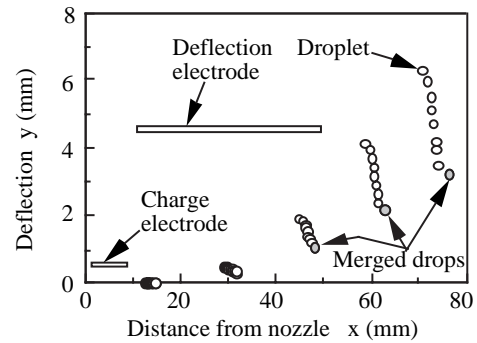
Analysis of Vertical-line Printing

1. Droplet-placement and Printed Image

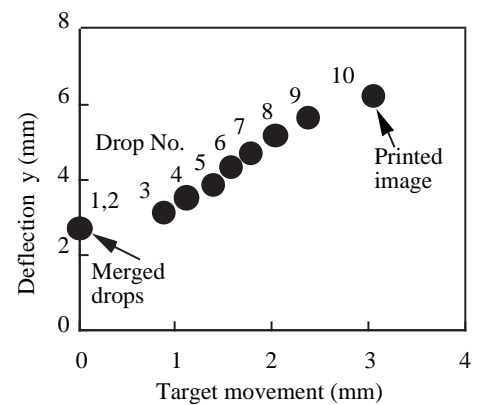
Droplet-placement and the predicted print image during vertical line printing are shown in Figure 10, as calculated by simulation according to the method discussed in the previous section. Droplet placement during line printing shows similar characteristics in observation (Figure 5) and simulation, such as merging of the first and second droplets, and delay of the last droplet. As a result of these factors, curved-line flight formation is also predicted. Furthermore, the curved bar-code print image that results from this curved flying formation also shows good agreement with the actual observed image in Figure 3. These results confirmed that this method of simulation can reproduce actual printing errors.

2. Force Applied to Droplets

To study placement errors, we investigated the changes in the forces exerted on the droplets as they fly, by cal-



1) Drop placement during printing of lines



2) Printed image

Figure 10. Drop placement and printing image during printing of lines (simulation)

culational and analysis. Figure 11 shows the force exerted (in the flying direction) on the first and the last droplet according to their distance from the nozzle.

The first droplet undergoes a large aerodynamic force due to drag after leaving the base-droplet layer and this reduces its flying velocity. On the other hand, the following droplet flies inside of wake that is formed by the preceding droplet, so the aerodynamic force is reduced and the decrease in flight velocity is smaller than in the case of the first droplet. Furthermore, the last droplet has no following droplet to apply forward-direction Coulomb force, so immediately after charging at the charge electrodes, only the backwards “braking” Coulomb force is applied and its flight velocity is therefore reduced more than that of any other droplet. As a result of these mechanisms, the same phenomena are observed in the situation as in the experiments, such as the second droplet catching up with the first droplet and merging, and the last droplet trailing far behind the other droplets.

3. Reduction of Droplet-Placement Error

Based on the results above, we will now discuss a method of reducing droplet-placement error. In order to re-

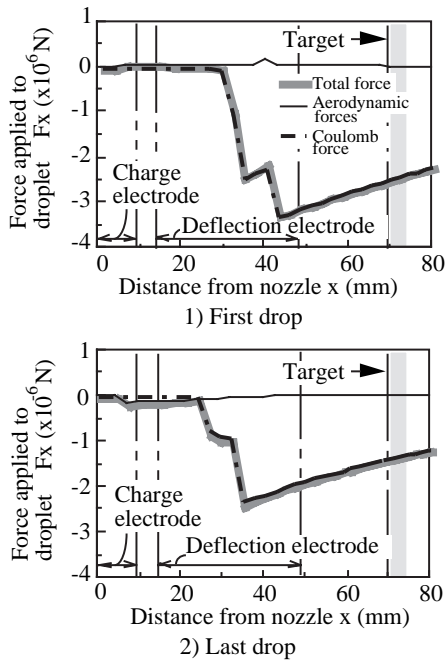


Figure 11. Forces applied to a droplet (simulation)

duce the effect of aerodynamic forces, decreasing flying distance and/or increasing droplet weight are both acceptable. On the other hand, to compensate for errors due to the Coulomb force, one might design a printing sequence that prints droplets from higher charge voltage to lower so as to provide back-up propulsion for the first droplet, which is subject to the greatest aerodynamic drag and to minimize the retarding Coulomb force on the last droplet.

Figure 12 shows the relationship between line-curvature ratio and working distance that, as obtained by experimentation and simulation. In this study, we evaluate line curvature is estimated using the “line curvature ratio”, defined as the ratio of deviation from the line to the diameter of the printing dot image. Good agreement between experiments and simulation was shown for every printing condition. Also, applying all of our countermeasure reduces the line-curvature ratio to 1/10 of the uncorrected value.

Conclusions

We have analyzed and observed the flight stability of droplets in an electrostatic ink-jet printer. The droplets are charged and fly near other particles, and thus interact with

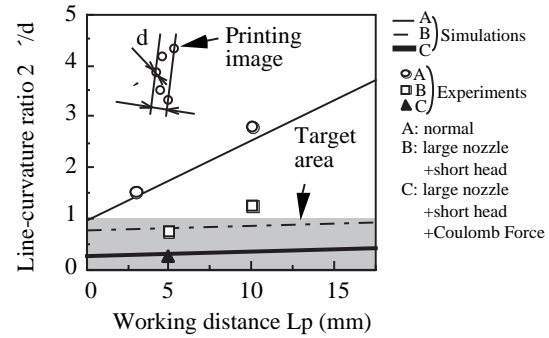


Figure 12. Relationship between line-curvature ratio and working distance

one another and deviate from their expected trajectories. These interactions are a major cause of droplet-placement error in high-speed printing. To understand the cause of such, we observed flying droplets, measured their charges, and modeled their flight dynamics using a simple system. That includes the effects of electrostatic repulsion and the interactions resulting from aerodynamic forces. Finally, a way to reduce the droplet-placement error was discussed and its effectiveness is confirmed.

References

1. G. L. Fillmore, W. L. Buehner and D. L. West, “Drop Charging and Deflection in an Electrostatic Ink Jet Printer”, *IBM J. Res. Develop.*, **21** (1977), pp. 37-47.
2. K. C. Chaudhary and L. G. Redekopp, “The Nonlinear Capillary Instability of a Liquid Jet-Part 1 Theory”, *J. Fluid. Mech.*, **96-2** (1980), pp. 257-274.
3. K. C. Chaudhary and T. Maxworthy, “The Nonlinear Capillary Instability of a Liquid Jet-Part 2 Experiments”, *J. Fluid. Mech.*, **96-2** (1980), pp. 275-286.
4. Y. Ebi and T. Kawamura, “Numerical Study of Droplet Formation from Liquid Jet”, *Ricoh Tech. Rep.*, **5** (1981), pp. 4-11.
5. A. Atten and S. Oliveri, “Charging of Drops Formed by Circular Jet Breakup”, *J. Electrostat.*, **29** (1992), pp. 73-91.
6. K. Asano, “Formation and Charging of Droplet Ejected from a Nozzle”, *Proceedings of the Institute of Electrostatics Japan.*, **18-1** (1994), pp. 18-24.
7. Tomita, *Hydraulics*, Jikkyo (1982).
8. Okamoto, *Applied Hydrodynamics*, Seibunndo (1968), pp. 150-152.
9. M. Horie and Y. Ebi, “Ink-Jet Printing and Charged Droplet”, *Proceedings of the Institute of Electrostatics Japan.*, **10** (1986), pp. 18-24.